Off-line method of the separation of the electrodes equilibrium state of the Li-ion batteries

Karrick Mergo Mbeya, Nicolas Damay, Guy Friedrich, Christophe Forgez, Maxime Juston

ELECTRIMACS 2019 – Salerno, Italy, 21st-23rd May 2019

Off-line method of the separation of the electrodes equilibrium state of the Li-ion batteries

K. Mergo Mbeya · N. Damay · G. Friedrich · C. Forgez · M. Juston

Abstract To ensure better performances of the Li-ion batteries in applications such as electric vehicles, the monitoring of their state with a BMS (Battery Management System) is required. To this end, non-invasive tools are needed to perform monitoring of the battery at the electrode scale. In this paper, we propose a method to extract from charge and discharge of the battery, the electrodes informations (equilibrium potentials, capacities and lithiation rates as functions of the battery state of charge). A pseudo-OCV model has been used to determine these informations. The proposed method allows to reduce the bias related to the battery overvoltage. Evaluated on a LFP/graphite lithium ion battery, the needed parameters were obtained with an accuracy of about 1 mV on the pseudo-OCV average (between discharge and charge) measurements of the battery. This method can be used for any battery chemestry.

1 Introduction

The Li-ion batteries (LIBs) are among the best energy storage systems offering higher power and energy density (at element scale, the energy density can reach 260 $Wh.kg^{-1}$), with a very low rate of self-discharge [1]. Thanks to these features, the LIBs are ubiquitous in various areas of use, from electronic devices to transport (electric vehicles, etc.). The use of ion lithium batteries in applications such as electric vehicles requires the monitoring of their state with a BMS (Battery Management System) to ensure the safety, better performances and a long lifespan.

K. Mergo Mbeya · N. Damay · G. Friedrich · C. Forgez · M. Juston
University of Sorbonne, University of Technology of Compiègne, CNRS, FRE 2012 Roberval,
Centre de recherche Royallieu, CS 60319, 60203 Compiègne Cedex, France
e-mail: karrick.mergo-mbeya@utc.fr, nicolas.damay@utc.fr

Classically, the LIBs monitoring is made by considering them as a "whole package", i.e. without any informations about its internal state [2]. In reality, a lithium ion cell consists of several internal elements including positive and negative electrodes, electrolyte and separator. Here we want to monitor the electrodes state of the LIB in odrer to bring a better control. An electrode state can be defined by many parameters and here we focus on the determination of their capacities and equilibrium potentials as a function of cell state of charge (SOC).

In this present paper, we propose a method to determine the electrodes state of the LIBS based on a pseudo-OCV model. The specificity of our method is to use the average measurements of the battery pseudo-OCV and the average reference curves of the equilibrium potentials of the electrodes. In section 2, we describe the composition of the pseudo-OCV of the LIBs. We also establish the mathematical equations which relate the parameters of the state of the electrodes with the pseudo-OCV. In section 3, we present the determination method of the electrodes parameter. In section 4, we evaluate the results of the method.

2 Characteristics of a LIB pseudo-OCV

2.1 Pseudo-OCV definition and modeling

The pseudo-OCV (pOCV) is defined as the battery voltage when its overvoltage (η) is equals a few tens of milivolts (i.e, at very low current) (Equation (1)) (Fig. 1) [3][4][5][7].

$$pOCV = OCV + \eta \tag{1}$$

where *OCV* (Open Circuit Voltage) represents the battery equilibrium voltage. The OCV varies with the battery state of charge (SOC) and the temperature T. This quantity is full of information (described in the next subsection), but difficult to measure (measuring OCV at differents battery SOC needs long time of rest during tests). The pOCV is often used in the litterature to save time.

The overvoltage η includes the contribution of internal various phenomena resulting in ohmic effects (transport of lithium ion in electrolyte and of electrons in electrodes, external electrical connectors, etc.) and dynamic effects (lithium charge-transfer and diffusion at each electrode). Please note here that apart from the current level, η is also impacted by the temperature, the SOC and the history of the battery (charge and discharge of the battery, and its state of health). This also leads to the variation of the *pOCV* with these parameters. Here we are particularly interested in its dependency on the SOC. Therefore, the other parameters are considered constant. SOC is calculed by the following formula : $SOC(t) = SOC_{init} + \int Idt$ [Ah]. SOC_{ini} is the initial state of charge, I is the measured current and t represents the time.

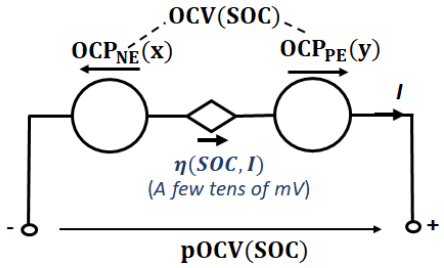

Fig. 1 Equivalent electric circuit model of the LIB.

2.2 Equilibrium voltage

2.2.1 Description

The battery OCV is the difference between the equilibrium potentials OCPs (OCP: Open Circuit Potential) of positive and negative electrodes (Equation (2)).

$$OCV(SOC) = OCP_{PE}(y) - OCP_{NE}(x). \quad (2)$$

where the subsrcipts PE and NE stand respectively for positive and negative electrodes. x and y are respectively the lithiation rates of the electrodes and are defined as follows:

- NE: $x = \frac{SOC_{NE}}{C_{NE}}$. SOC_{NE} (Ah) and C_{PE} (Ah) are respectively the state of charge and the capacity of the negative electrode (NE).
- PE: $y = \frac{SOC_{PE}}{C_{PE}}$. SOC_{PE} (Ah) and C_{PE} (Ah) are respectively the state of charge and the capacity of the positive electrode (PE).

The electrodes capacities are related to their specific design and electrochemical properties [6][7].

The electrode OCP is an electrical quantity measured at equilibrium state versus a reference electrode (metal lithium electrode (Li^+/Li) is mostly used as reference electrode). The electrode OCP varies non-linearly with the lithiation rate and with the history of the use of electrode (hysteresis) (see illustration on Fig. 2) [8]. The OCP curve can exhibit one or more plateaus which are theoretically related to the active material state at a given lithiation rate. The number of plateaus depends on the electrode chemical composition.

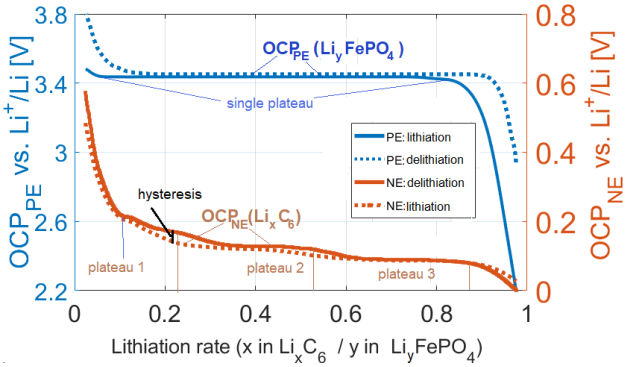

Fig. 2 Illustration of OCP vs. lithiation rate curves in the cases of positive Lithium-phosphate-Iron (Li_yFePO_4 or LFP) and graphite (Li_xC_6). The measurements were obtained against a lithium metal reference electrode (Li^+/Li). *Data source* [6].

2.2.2 Positions of the battery OCV-SOC and the electrodes OCP-lithiation rates curves in a real LIB

Fig. 3 illustrates the curves of electrodes OCP (vs. lithiation rates) and the battery OCV curves (vs. battery SOC) in a real LIB. It can be noted that when the battery SOC increases (during the charge of battery), x also increases and y decreases due to the transfer of ion lithium from postive electrode to negative electrode. (The reverse process occurs during the discharge of the battery). That is why the curve of the OCP_{PE} is reversed in Fig. 3 with respect to Fig. 2. C_{bat} (in Ah) is the battery capacity. Here C_{bat} is defined as the maximum value of SOC (at fully charged or discharged state of the battery).

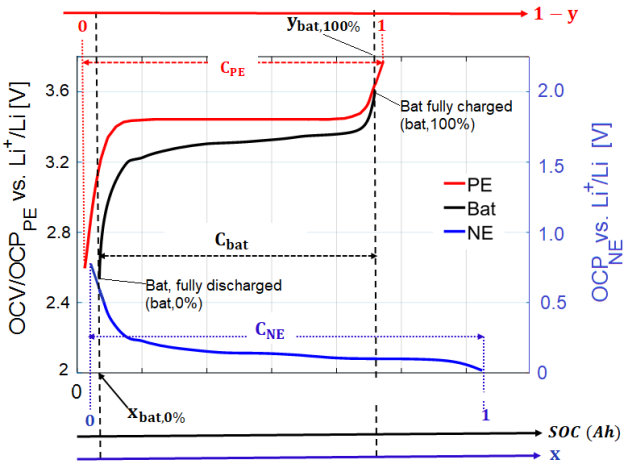

Fig. 3 Illustration of the positions of OCP_{PE}, OCP_{NE} and OCV curves in a LFP/graphite LIB [4][9].

$y_{bat,100\%}$ is the lithiation rate of the PE when the battery is fully charged (at $SOC_{max} = C_{bat}$). $x_{bat,0\%}$ is the lithiation rate of the NE when the battery is fully discharged (at SOC_{min}=0 Ah). Here the fully discharged and charged states of the battery correspond respectively to minimum (2.5 V) and maximum (3.6 V) limits of the battery voltage. Please note that for a real LIB, the electrodes cannot be fully used [4][9]. Therefore, when the battery is fully charged, the lithiation rate of PE $y_{bat,100\%}$ is close to 0 (i.e, $1 - y_{bat,100\%}$ is

close to 1, according Fig. 3). When the battery is fully discharged, the lithiation rate of NE, $x_{bat,0\%}$ is also close to 0. In general, the NE is designed with a capacity C_{NE} larger than the PE C_{PE} [9], as a result, the curve of OCP_{NE} (in Ah) is larger than the curve of OCP_{PE} (in Ah) as shown in Fig. 3. The oversized capacity of NE prevents its lithiation rate x to reach 1 in a real LIB. That avoids its OCP falls at 0 V Li^+/Li (see Fig. 3, at $x = 1$), which is the potential value of the unwanted reaction of the LIBs, called lithium plating [10,11].

From Fig. 3, the relationships between the battery SOC, x and y can be established. Thus, the battery SOC can be calculated with the equations (3) and (4).

$$SOC = (x - x_{bat,0\%})C_{NE}. \tag{3}$$

$$C_{bat} - SOC = (y - y_{bat,100\%})C_{PE}. \tag{4}$$

By expressing x and y based on SOC and other parameters, we obtain Eq.(5) and (6).

$$x = x_{bat,0\%} + \frac{SOC}{C_{NE}}. \tag{5}$$

$$y = y_{bat,100\%} + \frac{C_{bat} - SOC}{C_{PE}}. \tag{6}$$

Interestingly, from the equations (5) and (6) the electrodes OCP can be mathematically expressed as functions of the battery SOC. In addition, the electrodes OCP can be integrated to the pOCV expression by mixing the equations (2) and (1).

3 Method of identification of the electrodes state

In the previous section, it is clearly established that the parameters defining the state of the electrodes (OCP electrodes, $x_{bat,0\%}$, $y_{bat,100\%}$, C_{NE} and C_{PE},) are all included in the pseudo-OCV of the battery. For the determination of these parameters, only the discharging or charging measurements of the battery $pOCV$ and of the reference electrodes OCP curves could be used [7][12]. The parameters can be identified by a nonlinear least squares fitting. Here we propose to work on the average, between discharge and charge, of the measurements of the battery $pOCV$ and of the reference electrodes OCP curves. We think that the average of the pseudo-OCV (vs. SOC) is approximately equal to the average OCV (vs. SOC) ($pOCV_{avg} \simeq OCV_{avg}$), i.e, the contribution of the battery overvoltage is negligeable in the average pseudo-OCV. Before to discuss more about this aspect, we would like first to define the input data of our method and the objective cost function. The input data are defined as follow:

- The pseudo-OCV measurements vs. SOC of the studied battery in charge and discharge, which allow to have the average pseudo-OCV measurements ($pOCV^{meas}_{avg}(SOC)$).
- The reference curves of the OCP vs. lithiation rate of the electrodes in charge and discharge, which allow to have their averages ($OCP^{ref}_{PE,avg}(y^{ref})$ et $OCP^{ref}_{NE,avg}(x^{ref})$).

C_{bat} being known, the objective cost function f for identification of the unkown parameters ($\theta = [x_{bat,0\%}, y_{bat,100\%}, C_{NE}, C_{PE}]$) is defined as follow:

$$\begin{aligned} arg_\theta\ min\ f &= OCV^{est}_{avg} - pOCV^{meas}_{avg} \\ &= \left[OCP^{est}_{PE,avg} - OCP^{est}_{NE,avg}\right] \\ &- \left(OCV_{avg} + \frac{|\,\eta_{ch}\,| - |\,\eta_{dc}\,|}{2}\right)^{meas}. \end{aligned} \tag{7}$$

where θ represents the vector of parameters to identify. The term $\Delta\eta = \frac{|\eta_{ch}|-|\eta_{dc}|}{2}$ (Equation (7)) is considered as the source of bias. $\Delta\eta$ can be analyzed by observing the experimental data of the pOCV (C/50) and the OCV of a LFP/graphite in Fig. 4.

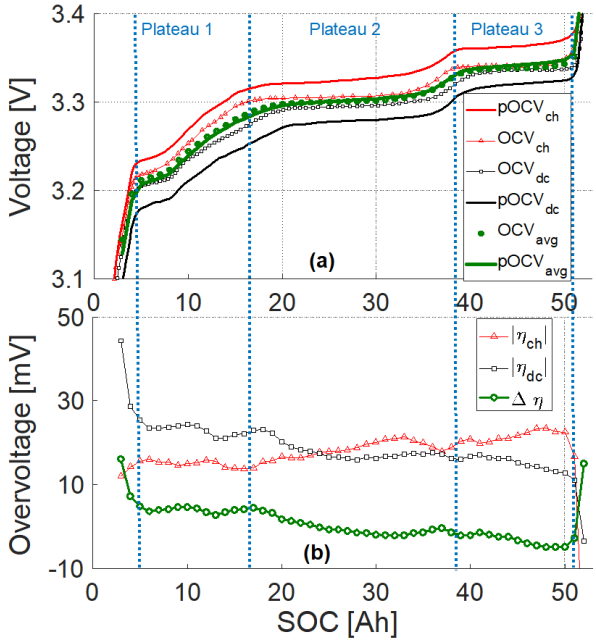

Fig. 4 (a) OCV and pOCV (C/50) measurement data in charge, discharge and the average between charge and discharge of a LFP/graphite LIB. b) The corresponding overvoltage.

From Fig. 4.(b), it can be observed that the overvoltage increases towards the low SOCs for discharge curve and the high SOCs for the charge curve. As a consequence, $\Delta\eta$ increases from both low and high battery SOCs. Focusing on only the region including the three plateaus (see Fig. 4.(a)) where the useful informations can be extracted, $\Delta\eta$ is three times smaller than the discharge and the charge overvoltage. Furthermore, one can observe the apparent shift of the plateaus between the $pOCV$ and the OCV curves for both discharge and charge. The shifts are considerably reduced by comparing the averages of $pOCV$ and OCV. This confirms the negligeable contribution of $\Delta\eta$ in the average $pOCV$ as it was expected.

The different steps of the algorithm are presented Fig. 5. The nonlinear least square optimization function *lsqnonlin*

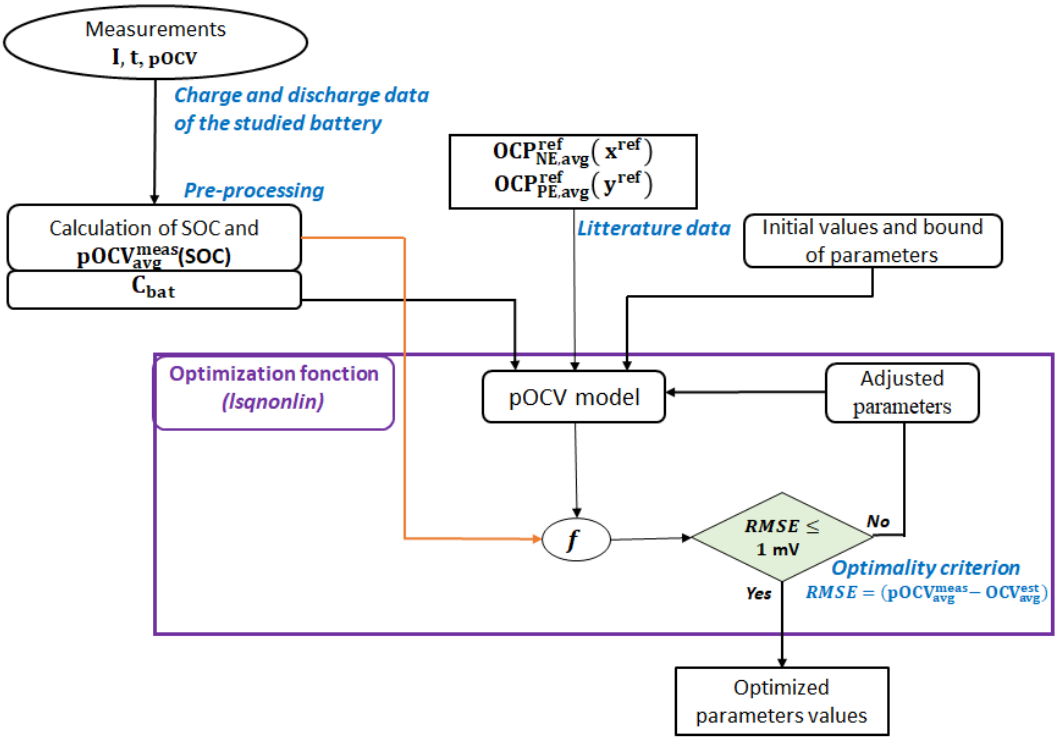

Fig. 5 Algorithm flowchart of the parameters identification. (RMSE: Root Mean Square Error).

on the Matlab software was used. The parameters $x_{bat,0\%}$ and, $y_{bat,100\%}$ are bounded between 0 and 1, and initialized to zero. C_{NE} and C_{PE} are initialized to C_{bat} and bounded as follow:

- for C_{NE} :between C_{bat} and $1.4C_{nom}$
- for C_{PE} :between C_{bat} and $1.2C_{nom}$

(C_{nom} is the battery capacity given by the manufacturer). The estimated electrodes OCPs as functions of the battery SOC are expressed in the following manner in the algorithm :

$$OCP_{PE,avg}^{est} = OCP_{PE,avg}^{ref}\left(y_{bat,100\%} + \frac{C_{bat} - SOC}{C_{PE}}\right). \quad (8)$$

$$OCP_{NE,avg}^{est} = OCP_{NE,avg}^{ref}\left(x_{bat,0\%} + \frac{SOC}{C_{NE}}\right). \quad (9)$$

4 Results and dicussions

To evaluate the proposed method, our study was carried out on the LIB A123Systems with a C_{nom} of 2.3 Ah and with a cylindrical form (size 18650). The cells consist of graphite negative electrode and LFP positive electrode. In the present study, the initial results of the pOCV measurements tests at charge C/25 (92 mA) and discharge at C/25 have revealed a battery capacity C_{bat} corresponding to about 93% of C_{nom}. These tests were performed at room temperature (25 °C) and by limiting the minimum and maximum voltage of cells respectively to 2.5 V and 3.6 V.

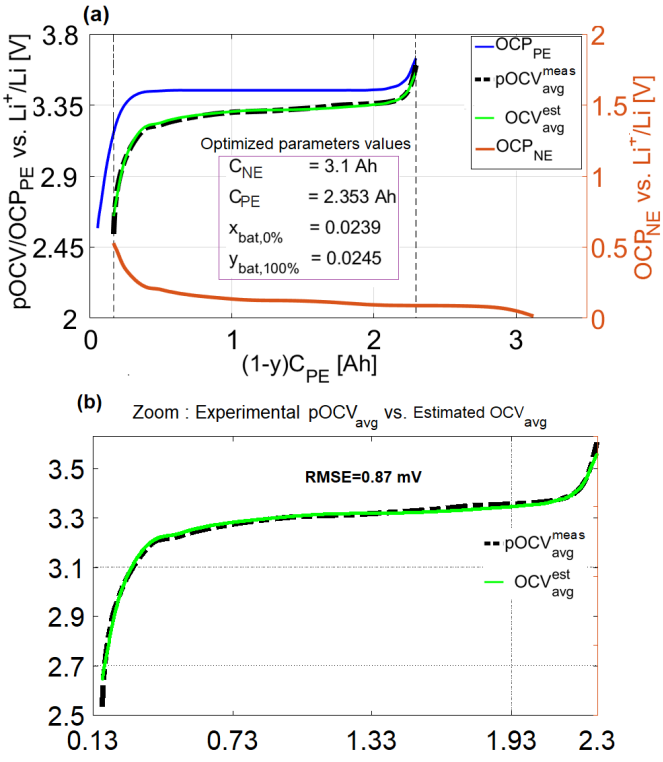

Fig. 6 (a) Experimental $pOCV_{avg}$ (black discontinuous curve) and the simulated OCV_{avg} profiles (green line) and average OCP curves of one of the studied cells. The estimated electrodes $OCP_{PE,avg}$ and $OCP_{NE,avg}$ curves are comprised between the two discontinuous vertical lines in black color. (b) Zoom of the experimental $pOCV_{avg}$ and the simulated OCV_{avg} profiles.

Fig. 6 shows the results of the application of the method in case of the studied cells. In Fig. 6.(a), the average

OCP curves of the electrodes of this battery correspond to the region between the two discontinuous vertical lines in black color. The estimated average OCV (OCV_{avg}^{est}) (green curve) represents the difference between the $OCP_{avg,PE}$ and $OCP_{avg,NE}$ curves in this region. From Fig. 6.(b), It can be observed that the slope between the last two plateaus being towards the high voltages is smoothed on the estimated OCV_{avg}^{est} profile, this because of the smoothing of the $OCP_{NE,avg}$ profile (see Fig. 6.(a)). In general, the profile of the estimated OCV_{avg}^{est} is closer to the average *pOCV* measurements. The root mean square error (RMSE) resulting between the average *pOCV* measurements and the estimated average OCV is less than 1 mV (about 0.87 mV), which is acceptable.

The obtained lithiation rates $x_{bat,0\%}$ and $y_{bat,100\%}$ are almost equal to 0.024 (value close to 0). The capacities C_{PE} and C_{NE} values are respectively 10% and 30% greater than the value of C_{bat}, (i.e, both positive and negative electrodes are not respectively used at about 10% and 30% in the battery). The value of C_{NE} is about 24% greater than C_{PE}.
From the physical point of view, we can note that the magnitude orders of these four parameters have a meaning. These values can be then used for determining the electrodes OCP as functions of the battery SOC for both charge and discharge from the reference curves of the electrodes OCP respectively, by using Equations (8) and (9).

5 Conclusions

This work presented a method to extract the electrodes equilibrium potentials, capacities and lithiation rates of real LIBs. The method uses a pseudo-OCV model, which allowed to determine these parameters by a nonlinear least squares fitting. This was achieved by working on the average (between charge and discharging) measurements of a LIB pseudo-OCV and the reference curves of the elecrodes OCP. The method was used on a commercial LFP/graphite LIB. And the results obtained are satisfactory in term of precision.

The proposed method can easily be used to diagnose the LIBs by following the evolution of the determined parameters during the battery lifespan. In particular, the change in the electrodes capacities (C_{PE} et C_{NE}) and lithiation rates ($y_{bat,100\%}$ and $x_{bat,0\%}$).

Acknowledgements We thank the ministry of national education of France and the region of Hauts-de-France for granting PhD research works.

References

1. J. Janek, Wolfgang G. Zeier, “A solid future for battery development.”, *Nature Energy*, vol. 1, pp. 16141, 2016.
2. W. Waag, C. Fleischer, D. U. Sauer “Critical review of the methods for monitoring of lithium-ion batteries in electric and hybrid vehicles.”, *Journal of Power Sources*, vol 258, pp 321-339, 2014.
3. M. Dubarry, V. Svoboda, R. Hwu, and B. Y. Liaw, “Incremental Capacity Analysis and Close-to-Equilibrium OCV Measurements to Quantify Capacity Fade in Commercial Rechargeable Lithium Batteries.”, *Electrochemical and Solid-State Letters.*, vol. 9, (10), A454-A457, 2006,
4. M. Dubarry, C. Truchot, B. Y. Liaw, “Synthesize battery degradation modes via a diagnostic and prognostic model.”, *Journal of Power Source*, vol.219, pp 204 -216, 2012.
5. M. Dubarry, N. Vuillaume, B. Y. Liaw “From single cell model to battery pack simulation for Li-ion batteries.”, *Journal of Power Sources*, Vol.186 (2),pp. 500-507, 2009.
6. E. Prada, D. Di Domenico, Y. Creff, J. Bernard, V. Sauvant-Moynot, F. Huet, “Simplified Electrochemical and Thermal Model of LiFePO4-Graphite Li-Ion Batteries for Fast Charge Applications”, *Journal of Electrochemical Society* vol. 159, A1508-A1519, 2012.
7. T. Lu, Y. Luo, Y. Zhang, W. Luo, L. Yan, J. Xie, “Degradation Analysis of Commercial Lithium-Ion Battery in Long-Term Storage.”, *Journal of The Electrochemical Society*, vol. 164 (4), A775-A784, 2017.
8. W. Dreyer, J. Jamnik, C. Guhlke, R. Huth, J. Moskon, M. Gaberscek, “The thermodynamic origin of hysteresis in insertion batteries.”, *Nature Materials*, vol. 9, pp 1-6, 2010.
9. C. R. Birkl, M.R. Roberts, E McTurk, P G. Bruce, D. A. Howey, “ Degradation diagnostics for lithium ion cells.”, *Journal of Power Sources*, vol. 341, pp. 373-386, 2017.
10. P. Arora, M. Doyle, R. E. White,“ Mathematical Modeling of the Lithium Deposition Overcharge Reaction in Lithium-Ion Batteries Using Carbon-Based Negative Electrodes.”, *Journal of Electrochemestry Society*, vol. 146,(10), 3543-3553, 1999.
11. T. Waldmann, B.I Hogg, M. Wohlfahrt-Mehrens,“Li plating as unwanted side reaction in commercial Li-ion cells – A review.”, *Journal of Power Sources*, vol. 384, 107–12, 2018.
12. X. Han, M. Ouyang, L. Lu, J. Li, Y. Zheng, Z. Li, “A comparative study of commercial lithium ion battery cycle life in electrical vehicle: Aging mechanism identification.”, *Journal of Power Source*, vol. 251, pp. 38-54, 2014.